Journal of Medicinal Chemistry

Article

pubs.acs.org/jmc

# Thiazolylaminomannosides As Potent Antiadhesives of Type 1 Piliated *Escherichia coli* Isolated from Crohn's Disease Patients

Sami Brument,[†] Adeline Sivignon,[‡,§] Tetiana I. Dumych,[⊥] Nicolas Moreau,[†] Goedele Roos,[#] Yann Guérardel,[▽] Thibaut Chalopin,[†] David Deniaud,[†] Rostyslav O. Bilyy,[⊥,*] Arlette Darfeuille-Michaud,[*,‡,§,∥] Julie Bouckaert,[*,▽] and Sébastien G. Gouin[*,†]

[†]LUNAM Université, CEISAM, Chimie Et Interdisciplinarité, Synthèse, Analyse, Modélisation, UMR CNRS 6230, UFR des Sciences et des Techniques, 2 rue de la Houssinière, BP 92208, 44322 NANTES Cedex 3, France

[‡]Clermont Université, UMR 1071 Inserm/Université d'Auvergne, 63000 Clermont-Ferrand, France

[§]INRA, Unité Sous Contrat 2018, 63000 Clermont-Ferrand, France

[∥]Centre Hospitalier Universitaire, 63000 Clermont-Ferrand, France

[⊥]Institute of Cell Biology, National Academy of Sciences of Ukraine, Lviv, Ukraine

[#]Algemene Chemie (ALGC), Vrije Universiteit Brussel, Brussels, Belgium

[▽]Unité de Glycobiologie Structurale et Fonctionnelle (UGSF), UMR8576 du CNRS, Université Lille 1, F-59655 Villeneuve d'Ascq Cedex, France

Supporting Information

**ABSTRACT:** Adherent-invasive *Escherichia coli* (AIEC) have previously been shown to induce gut inflammation in patients with Crohn's disease (CD). We developed a set of mannosides to prevent AIEC attachment to the gut by blocking the FimH bacterial adhesin. The crystal structure of the FimH lectin domain in complex with a lead thiazolylaminomannoside highlighted the preferential position for pharmacomodulations. A small library of analogues showing nanomolar affinity for FimH was then developed. Notably, AIEC attachment to intestinal cells was efficiently prevented by the most active compound and at around 10000-fold and 100-fold lower concentrations than mannose and the potent FimH inhibitor heptylmannoside, respectively. An ex vivo assay performed on the colonic tissue of a transgenic mouse model of CD confirmed this antiadhesive potential. Given the key role of AIEC in the chronic intestinal inflammation of CD patients, these results suggest a potential antiadhesive treatment with the FimH inhibitors developed.

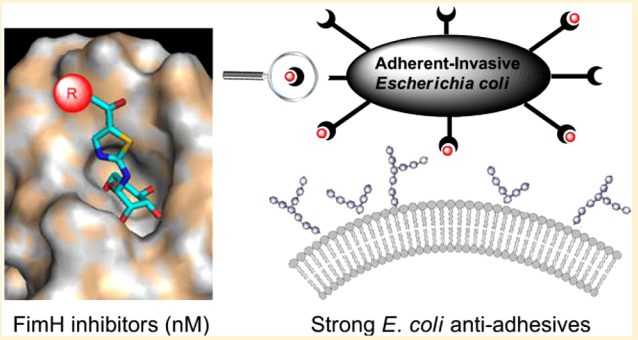


## INTRODUCTION

Crohn's disease (CD) is characterized by an aberrant immune response occurring in a genetically predisposed host in response to microbes and/or microbial compounds.[1,2] In patients with CD, high concentrations of bacteria forming a biofilm on the surface of the gut mucosa and increased numbers of mucosa-associated *Escherichia coli* are observed.[3] These bacteria, called AIEC for adherent-invasive *E. coli*, colonize the ileal mucosa of CD patients.[4] They can adhere to intestinal epithelial cells and replicate rapidly within macrophages and epithelial cells inducing the secretion of large amounts of TNF-$\alpha$.[5] For CD patients in whom the ileum is involved in the disease, an abnormal expression of carcinoembryonic antigen-related cell adhesion molecules 5 and 6 (CEACAM5 and CEACAM6) has been reported and studies have shown that CEACAM6 acts as a receptor for AIEC bacteria.[6] The host/bacteria crosstalk in the context of host susceptibility to CD was mimicked using a transgenic mouse model expressing human CEACAM6 receptor. AIEC-infected mice were abundantly colonized by these bacteria and developed severe colitis.[7]

As AIEC attachment is mediated by the FimH adhesin located at the tip of the type 1 pili, which bind to oligomannosides displayed on intestinal cells, we hypothesized that the development of FimH antagonists preventing AIEC binding to the gut could be relevant for CD treatment. Such an antiadhesive strategy based on FimH inhibition has attracted much attention during the past few years for the treatment of urinary tract infections (UTIs). We and others have developed synthetic mannosides with promising in vitro[8,9] and in vivo[10,11] antiadhesive potencies. Increased affinity for FimH was

Received: February 21, 2013

   dx.doi.org/10.1021/jm400723n | J. Med. Chem. XXXX, XXX, XXX−XXX

obtained with synthetic *O*-mannosides bearing hydrophobic aglycons interacting with two tyrosines (Tyr48 and Tyr137) at the entrance of the FimH binding site.

The aim here was to develop a new class of FimH antagonists bearing *N*-linked heterocyclic aglycons. *N*-Mannosides have been much less investigated for FimH inhibition.[12,13] The aromatic heterocycles should increase the binding affinity through stacking interactions with Tyr48 and Tyr137 of FimH. Water solubility issues, generally encountered with *O*- or *C*-mannosides bearing hydrophobic aglycons, may also be reduced. We selected two heterocycles (pyrimidine and thiazole) which are accessible by a convenient addition-cyclization methodology developed in our group.[14] In view of the broad adaptability of the FimH binding site, illustrated by the numerous FimH antagonists based on *O*- or *C*-linked mannosides described so far,[8−11] we hoped for a first hit with one of the lead heterocyclic mannosides. We then planned to improve the FimH binding potency by designing a small library of a second generation of inhibitors with different pharmacophores on the heterocycle.

Thiazole was the only heterocycle to be further considered as pyrimidine-based mannosides adopted an unusual $^1C_4$ configuration, unsuitable for FimH inhibition. Co-crystallization of a lead compound with FimH showed possible pharmacomodulations of the $R_2$ group (Scheme 1) to give supplementary

**Scheme 1. Structure of the Mannosides with Pyrimidine and Thiazole Aglycons**

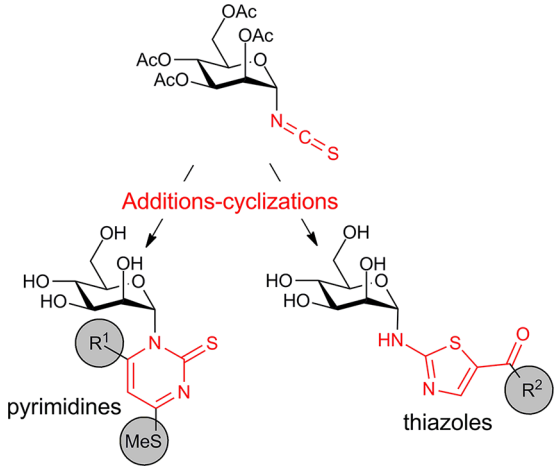


stacking interactions with Tyr48. A small library of analogues was then designed, and the binding potency on FimH evaluated by a competitive enzyme-linked immunosorbent assay (ELISA). The ability of the new FimH antagonists to prevent adhesion of the AIEC reference strain LF82 was assessed in vitro with guinea pig erythrocytes and the human intestinal cell line T84 and ex vivo in the colonic loop of a transgenic mouse model of CD.

## RESULTS AND DISCUSSION

**Synthesis.** The selected heterocycles would be poorly grafted on sugars by conventional glycosylation methods due to the presence of nucleophilic heteroatoms. Thus, the pyrimidine and thiazole rings were built by an addition-cyclization methodology developed in our group, performed here on mannosylisothiocyanate (Scheme 1). Interestingly, this chemical procedure enabled a library of analogues to be generated by conducting the cyclization step with dienes or dienophiles bearing diverse R groups. We have also previously shown that the thiomethyl group of the pyrimidine ring can easily be substituted by nucleophilic displacement,[15] which provides further opportunities to increase the chemical diversity of the heterocycles.

Our efforts were first focused on the pyrimidine series. Peracetylated mannosylisothiocyanate **1**[16] was obtained from the corresponding mannopyranosylchloride[17] with potassium thiocyanate and tetrabutylammonium iodide, as previously described by Camarasa and co-workers.[18] This compound was engaged in a [4 + 2] cycloaddition reaction with 1,3-diazadienum iodide[19] **2** and triethylamine to afford the pyrimidine **3** in a quantitative yield (Scheme 2). The cyclization

**Scheme 2. Synthesis of the Pyrimidylmannosides 4 and 5**

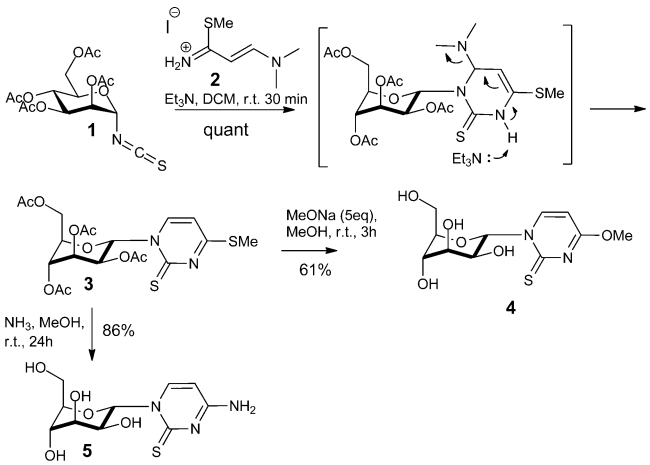


step was followed by a spontaneous deamination and the intermediate presented in Scheme 2 was never isolated. $^1H$ NMR analysis revealed a surprisingly high $H_1-H_2$ coupling constant for a mannoside of $J_{1,2}$ = 9.6 Hz (Supporting Information Figure S1), not in agreement with the generally observed $^4C_1$ conformation but coherent with the less frequently observed $^1C_4$. This assumption was further confirmed by the crystallographic structure of compound **3** (Figure 1).

The thiomethyl group of **3** was shown to be sensitive to nucleophilic substitution. An excess of sodium methanolate or ammonia in methanol led to unprotected compounds **4** and **5** where the thiomethyl group was substituted by a methoxy and an amino group, respectively. Both compounds retained the unusual $^1C_4$ conformation during the deprotection steps. Pyrimidine-based analogues were not further developed because the $^1C_4$ conformation adopted by the mannose hinders an optimal fit in the FimH binding site. In fact, compounds **3** and **4** were poor inhibitors of FimH in a cell-based assay (results not shown). It should be noted that previously described FimH inhibitors based on triazolylmethyl-*C*-mannosides adopting a $^1C_4$ conformation also displayed a relatively low affinity for FimH.[13]

The addition-cyclization strategy was then used to build the thiazole on mannose. Mannosylisothiocyanate **1** was first reacted with $NH_3$ gas in toluene to form thiourea derivative **6** in 92% yield without deacetylation of the sugar moiety (Scheme 3). Compound **6** was quantitatively converted into the thiazadiene **7** with *N*,*N*-dimethylformamide dimethyl acetal


dx.doi.org/10.1021/jm400723n | J. Med. Chem. XXXX, XXX, XXX−XXX

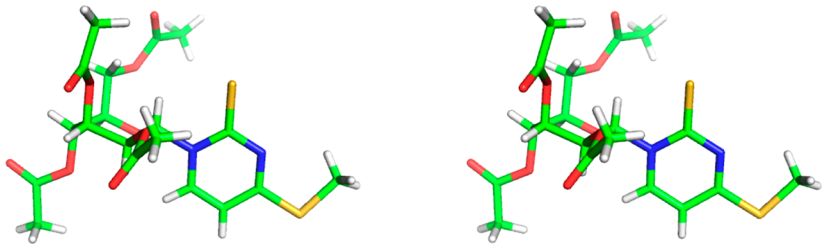

**Figure 1.** Crystallographic structure of compound **3** showing the unusual $^{1}C_{4}$ conformation.

**Scheme 3. Synthesis of Aminothiazole 9**

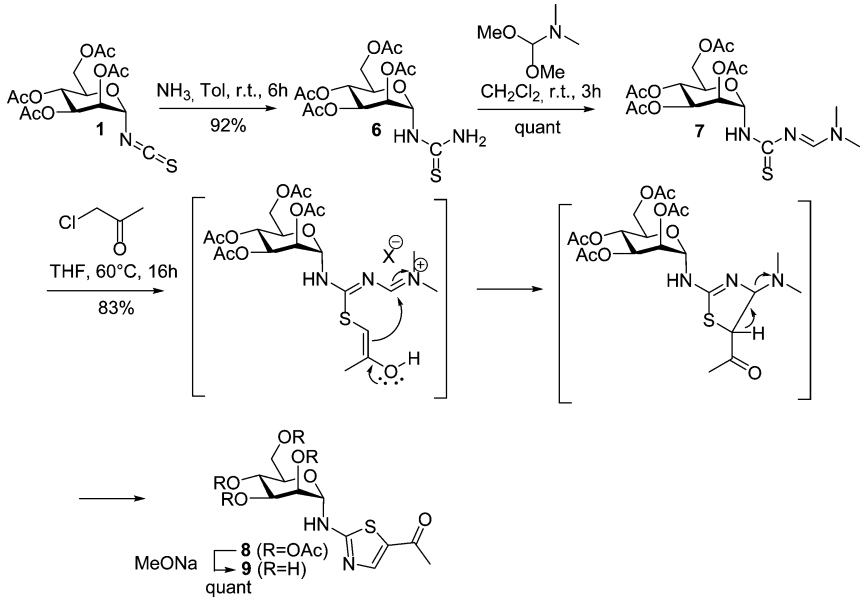


**Scheme 4. Structure of the Thiazolylaminomannosides 10−31**

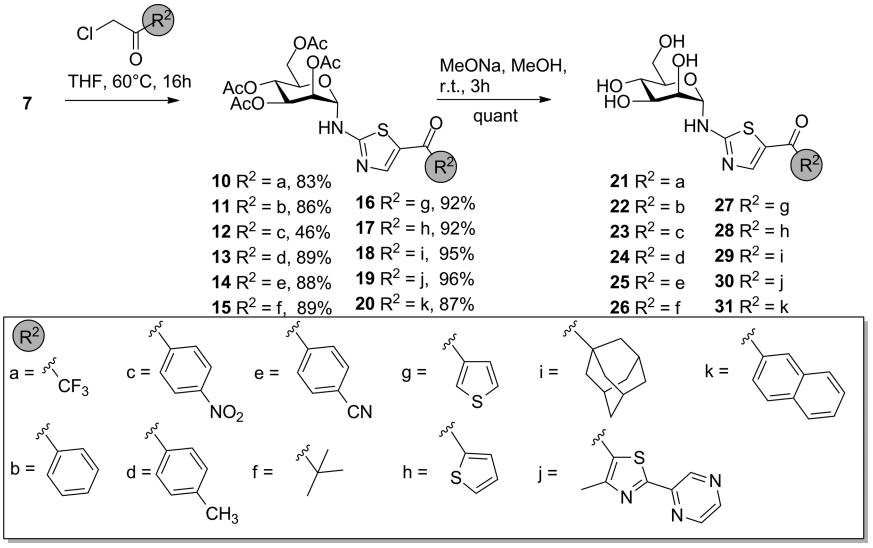


(DMFDMA) in dichloromethane. The subsequent addition-cyclization reaction was first performed with a 2-fold excess of 1-chloropropan-2-one and triethylamine at 60 °C for 16 h. Under these conditions, compound **8** was obtained in 83% yield as a pure $\alpha$-anomer (Scheme 3). Experimental conditions must be carefully controlled as increasing both the reaction time to 48 h and the temperature to 70 °C led to the formation of the $\beta$-anomer in a proportion reaching up to 50%. $\alpha$- and $\beta$-anomers were unambiguously identified with the critical anomeric $^{1}H-^{13}C$ $^{1}J$ coupling constants, which have previously been shown to be around 170 Hz for $\alpha$-products and 150 Hz for $\beta$-products.[20] The values observed for a mixture of $\alpha$- and $\beta$-anomers **8**, obtained with increased reaction times, were 166 and 149 Hz, respectively (Supporting Information Figure S2). The deprotection of the $\alpha$-anomer was carried out with only


dx.doi.org/10.1021/jm400723n | J. Med. Chem. XXXX, XXX, XXX−XXX

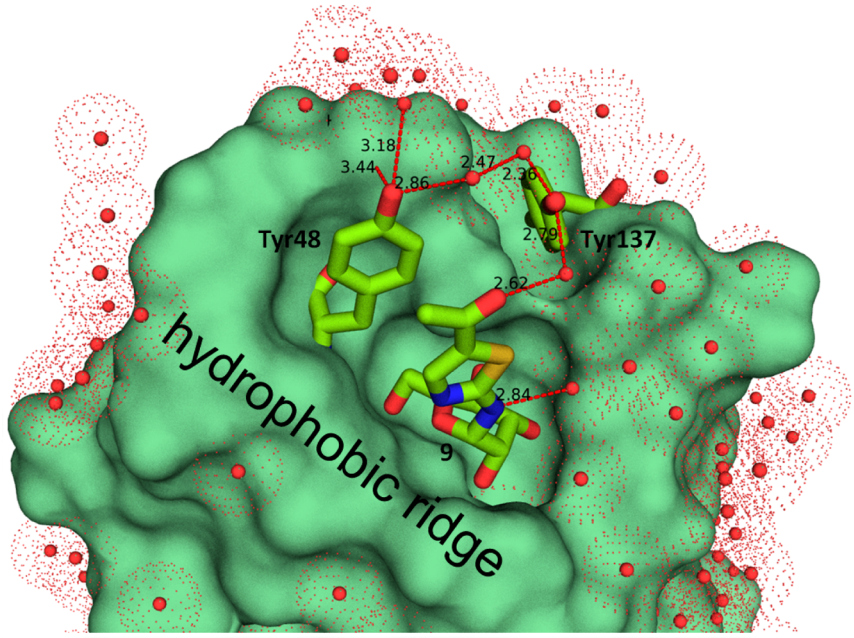


**Figure 2.** FimH−**9** complex showing the ligand **9** bound with its thiazole stacked against the closed tyrosine gate. The same overall structure, with Tyr48 and Tyr137 and **9** (all shown in ball-and-stick model), is observed in the crystals in both the orthorhombic and the monoclinic space groups (PDB entry codes 3zl1 and 3zl2). Water molecules are shown as red-dotted spheres expanding to their van der Waals radius (figure created using Pymol version 0.99). The figure shows hydrous solvation over Tyr137 and hydrophobic shielding of the tyrosine gate. Polar interactions (in Å) are also displayed and a crown of water rendering Tyr137, Tyr48, and the carboxylate of **9** with the solvent.

0.05 equiv of sodium methanolate in methanol to give the expected compound **9** quantitatively.

The promising binding affinity of **9**, and insights into the interaction with the FimH lectin domain provided by the crystallographic structure (see following sections), encouraged us to design a small library of analogues with an aromatic $R^2$ group (Scheme 1). This was achieved by selecting commercial $\alpha$-halogenoketones (8 out of 11 with an aromatic group) for the cyclization step. The second generation of thiazolylamino-mannosides **21**−**31** was obtained with excellent overall yields ranging from 83 to 96% (except for **23**) for the addition-cyclization and deprotection steps (Scheme 4). In each case, the reaction was over after 16 h and the lower yield observed for **12** (46%) was attributed to a more difficult purification. The anomeric substituents of the unprotected compound were shown to be in dynamic equilibrium in water with a preference for the $\alpha$ forms ($\alpha/\beta$ ratio >3/1, except for **28**, $\alpha/\beta$ = 3/2).

**Crystal Structure of the FimH Lectin Domain in Complex with Thiazolylaminomannoside 9.** The lead compound **9** was cocrystallized with the FimH lectin domain to investigate the influence of the thiazole and to define the relevant positions for complementation binding in the hydrophobic tyrosine gate of FimH.

Crystallization was accomplished using the sitting drop vapor diffusion method in two different space groups, orthorhombic and monoclinic (Supporting Information Table S1). The structure in the monoclinic space group was refined to 1.55 Å resolution and contains two complexes in the asymmetric unit; 339 water molecules could be identified in their electron density. All three FimH−**9** complexes are almost identical and show the ligand **9** bound with its thiazole stacked against the closed tyrosine gate (Figure 2).

The aromatic side chain of Tyr48, the first gate door residue, shows a parallel orientation with the thiazole ring of **9** at a distance of about 3.7 Å. However, these two aromatic groups are not perfectly stacked for an optimal interaction (Figure 3). The staggered orientation places the methyl of **9** at the *C*2 axis of symmetry of the phenyl ring of Tyr48. Thus, we hypothesized that the substitution of the methyl group of **9** by an aromatic substituent should enable further stacking interactions with the side chain of Tyr48. Furthermore, Tyr48 forms part of a nonhydrated ridge which is a hydrophobic extension of the binding site of FimH in the tip of the protein (Figure 2). For these reasons, the methyl position was favored for carrying out pharmacomodulations (i.e., compounds **21**−**31**) with aromatic or hydrophobic substituents to increase FimH binding affinity.

Tyr137, the second gate door residue, faces the solvent on the exterior of the protein and shields the mannose-binding site from solvent. The electron density of the sulfur atom in **9** is oriented toward the distant, orthogonally stacked Tyr137 residue (Figure 3A). Although this polarization of the sulfur atom in **9** toward Tyr137 does not appear to contribute to binding (positive $E_{int}$ for **9**−Tyr137 in Table 1), it seems to alleviate significantly the electronic hardness ($\eta$ ($r$) in Table 1), thus favoring the interaction of **9** with both tyrosine gate doors.

**Quantum Chemical Calculations.** A relaxed potential surface scan for the rotation of the carbonyl moiety around the C−C bond connecting the carbonyl and the thiazole in ligand **9** (Figure 4) determined that the carbonyl group of **9** is in its lowest energy state in the crystal structure of the FimH−**9** complex. The methyl group is on the opposite side of the sulfur of the thiazole and, in this orientation, the acetyl is in an excellent position to interact with Tyr48 (Figure 3).

The interaction energy between ligand **9** and Tyr48 and Tyr137 was then calculated and compared with that of benzene located at the same position as the heterocycle of ligand **9** as the reference molecule. The total interaction energy between


dx.doi.org/10.1021/jm400723n | *J. Med. Chem.* XXXX, XXX, XXX−XXX

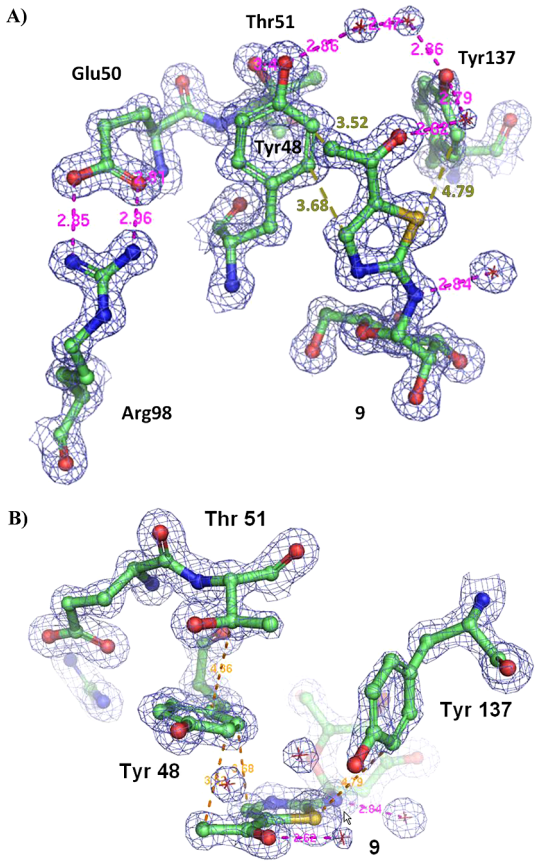


**Figure 3.** Two different views of ligand **9** in the mannose-binding site of FimH. The hydrophobic stacking of **9** against the closed tyrosine gate (distances in Å) shows its sulfur atom pointing toward Tyr137 and the parallel but staggered orientation of the thiazole ring of **9** relative to the phenyl group of Tyr48.

**Table 1. Interaction Energies $E_{int}$, Local Hardness $\eta$ ($r$), and Polarizabilities $\alpha$, of the Thiazolyl Moiety of 9 and Benzene**

| | thiazolyl of **9** | | benzene | |
|---|---|---|---|---|
| global | Tyr137 + Tyr48 | | Tyr137 + Tyr48 | |
| $E_{int}$ (kcal/mol) | −5.1 | | −3.0 | |
| $\alpha$ (bohr$^3$) | 99 | | 41 | |
| local | Tyr137 | Tyr48 | Tyr137 | Tyr48 |
| $E_{int}$ (kcal/mol) | 0.1 | −5.1 | −0.4 | −2.6 |
| $\eta$ ($r$) (kcal/mol) | 46 | 58 | 95 | 104 |

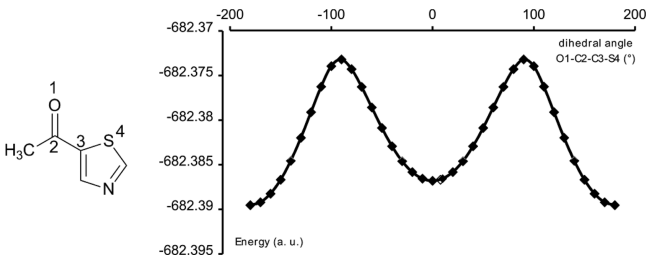


**Figure 4.** Scan orientation of the carbonyl group.

ligand **9** and both Tyr137 and Tyr48 is −5.1 kcal/mol, while that of benzene is only −3.0 kcal/mol (Table 1), explaining the high affinity of ligand **9**.

To obtain a more detailed picture, the individual interaction energies between ligand **9** (or benzene) and Tyr137 or Tyr48 were calculated. For both ligands, the interaction with Tyr48 is the strongest, while that with Tyr137 is negligible (Table 1). This can be related to the structure in which Tyr48 is found to be closer to the ligand, and in parallel, than Tyr137, which is oriented in a T-shaped stacking position.

In addition, the dispersion and the electrostatic energy components of the interactions between the ligand and Tyr137 and Tyr48 were determined. From a conceptual point of view, the dispersion energy can be related to the polarizability ($\alpha$) and the electrostatic energy to the local hardness ($\eta$ ($r$)).[21] The polarizability $\alpha$ is a global descriptor, giving an estimation of the dispersion component of the total interaction energy between ligand **9** or benzene and both Tyr137 and Tyr48. $\alpha$ is the tendency of an electron cloud to be distorted by an electric field caused, for example, by the stacking partner. A larger polarizability is favorable for the interaction. A polarizability of 99 bohr$^3$ was found for ligand **9**, while that for the reference molecule benzene was 41 bohr$^3$. This result corresponds to the more favorable interaction energy found for ligand **9**.

The local hardness is a measure of negative charge accumulation and is a local descriptor giving an estimation of the electrostatic component of the interaction energy at localized points. A large value of $\eta$ ($r$) indicates a high repulsion energy and thus an unfavorable interaction energy. Local hardness should only be compared at the same points (Supporting Information Figure S3). For the interaction with Tyr48, a local hardness of 58 and 104 kcal/mol was found for ligand **9** and benzene, respectively. This corresponds to the more favorable interaction energy of 2.5 kcal/mol calculated between ligand **9** and Tyr48. For the interaction with Tyr137, a local hardness of 46 and 95 kcal/mol was found for ligand **9** and benzene, respectively. This large difference in local hardness is not reflected in the interaction energies calculated between the ligands and Tyr137. Taken together, the relatively high polarizability and low local hardness of ligand **9** can explain its high affinity.

**Binding Affinity for FimH.** The binding affinity of the synthetic thiazolylaminomannosides **9** and **21**−**31** toward FimH was first evaluated by competitive ELISA. Heptylmannoside (HM) was also included in the assay as a reference displaying a strong nanomolar affinity for FimH.[22] The RNaseB protein, which possesses a complex mixture of oligomannose glycans ($Man_5GlcNAc_2$, $Man_7GlcNAc_2$, and $Man_8GlcNAc_2$),[23] was used as the FimH substrate (Figure 5). The intensity of FimH binding to the substrate is represented by the optical density of chromophore absorbance at 450 nm and decreases in the presence of inhibitors in a dose-dependent manner. The thiazolylaminomannosides **9** and **21**−**31** showed a strong affinity for FimH. Compared to the control (FimH alone), most of the inhibitors, including HM, already significantly inhibited FimH binding at 5 nM. The marked signal reduction obtained with HM at nanomolar concentrations is consistent with the low dissociation constants of 5[22] and 7 nM[24] previously reported for the HM-FimH complex by surface plasmon resonance (SPR) and isothermal titration calorimetry (ITC), respectively. Different inhibitory profiles were observed depending on the nature of the substituents attached to the thiazole ring. This clearly shows that improved affinity for FimH may still be expected with pharmacophores situated at rather large distances from the mannose binding site. As can be seen from Figure 5, thiazolylaminomannosides **22** and **30** were able to block FimH binding toward oligomannose glycans at the low concentration of 5 nM, while mannosides **21**, **24**, **26**,


dx.doi.org/10.1021/jm400723n | J. Med. Chem. XXXX, XXX, XXX−XXX

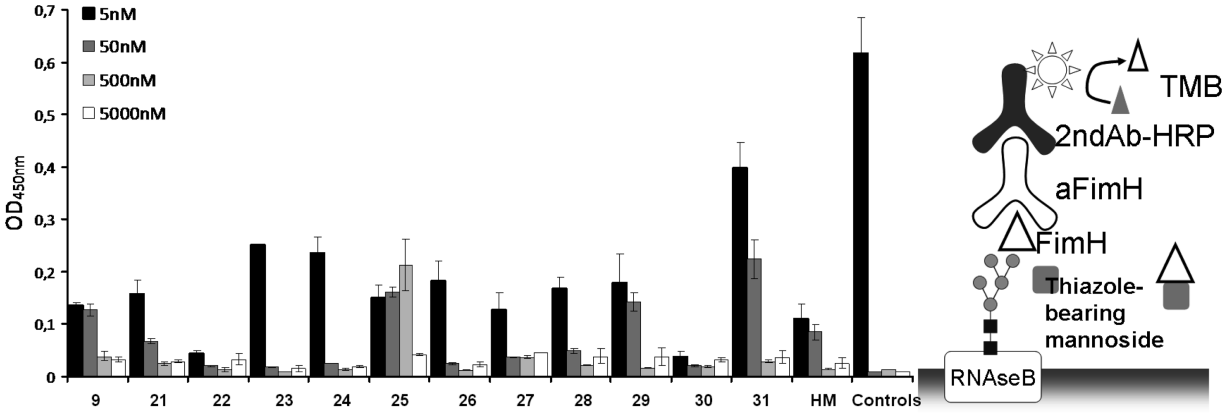


**Figure 5.** Affinity testing of thiazolylaminomannosides toward oligomannose glyco-epitopes using enzyme-linked immunosorbent assay (ELISA). The *X*-axis indicates the compounds used for testing; the *Y*-axis represents the optical density of TMB chromophore absorbance at 450 nm. The controls are (from left to right): FimH alone (positive control, black bar), aFimH (dark-gray bar), aFimH + 2ndAb-HRP (light-gray bar), 2ndAb-HRP (white bar), and TMB (negligible, not shown). The schematic principle of the assay is shown on the right. Briefly, oligomannose glycans of RNaseB (as the best suited natural FimH target) and the studied inhibitors compete for binding of FimH lectin, then bound FimH is detected by antibodies. In the case of the absence of inhibitor or a weak inhibitor, FimH will bind to RNaseB sorbed onto a plate and will produce a high signal of absorbance, while a strong inhibitor will bind to FimH and prevent it from binding to RNaseB on a plate, resulting in a low optical density signal.

**27**, and **28** effectively blocked its binding at a higher concentration of 50 nM. A significantly higher level of inhibition was observed with **22** and **30** compared to the HM reference.

**Prevention of Bacterial Attachment to Erythrocytes.** A widely used cell-based assay (hemagglutination, HAI) was first selected to evaluate the antiadhesive potency of the glycoconjugates **9** and **21**–**31** toward the CD-associated *E. coli* strain AIEC LF82. AIEC adhesion to the gut occurs through the binding of FimH adhesins to the mannosylated glycans of intestinal cells. This scenario was first mimicked here with the highly mannosylated glycocalyx of guinea pig erythrocytes.

A 2-fold dilution series of the antagonists was added to wells containing guinea pig erythrocytes and AIEC LF82 bacteria. The formation of the cross-linked network (hemagglutination) due to the interaction of the *E. coli* FimH adhesins with the glycocalyx of the erythrocytes was prevented at a certain concentration of inhibitors. The lowest concentration at which hemagglutination is still inhibited is defined as the inhibition titer of the antagonist. HM was included in the assay to obtain a relative inhibitory concentration (rIC) for the antagonists by dividing the inhibitory concentration (IC) of the substance of interest by the value for HM. In fact, rICs are more accurate than rough inhibition titers to compare the potency of antagonists evaluated in different assays.

HAI titers confirmed the good to excellent inhibitory potencies of the thiazole antagonists. Analogues less potent than HM in this assay were **9**, **21**, and **31** (Figure 6). Antagonist **21**, bearing the highly electron-withdrawing group $CF_3$, was significantly less potent than **9** with the $CH_3$ group. The same tendency was also observed in the aromatic series. Compounds **23** and **25** with $NO_2$ and CN groups were less potent than the unsubstituted phenyl analogue **22**. The electron-withdrawing groups probably hamper interactions with the Tyr48 side chain. Alkyl-armed thiazoles **9** and **26**, bearing a methyl and a *tert*-butyl group, showed a similar inhibitory profile to HM. A significant improvement was observed with compound **29** bearing a bulky adamantyl group. The most potent FimH inhibitor **30**, identified in the ELISA,

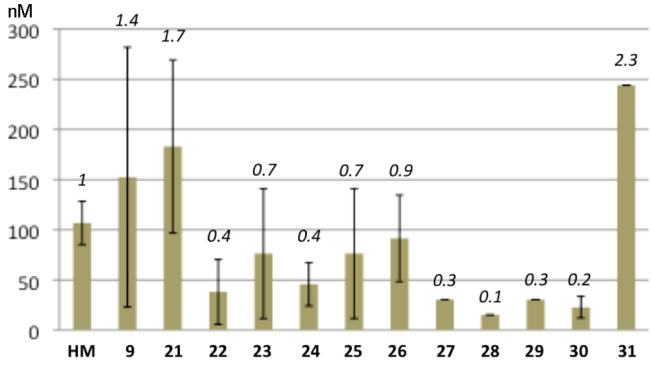


**Figure 6.** Inhibition of hemagglutination (HAI): inhibition of guinea pig red blood cell hemagglutination by the type-1 piliated AIEC strain LF82 by the newly synthesized glycoconjugates. The error bars indicate the variation in inhibitory concentrations (ICs, in nM) for the two assays with variable *E. coli* LF82 bacterial numbers. rICs relative to HM are indicated in italic.

was also shown to be the second most potent compound to prevent AIEC attachment to guinea pig erythrocytes.

**Prevention of Bacterial Attachment to Intestinal Epithelial Cells T84.** The capacity of the inhibitors to prevent adhesion of the AIEC bacteria to intestinal epithelial cells was then evaluated. This assay is particularly relevant because T84 cells highly express CEACAM6, a receptor for AIEC bacteria, reflecting the aberrant expression of CEACAM6 in the ileal mucosa of CD patients.

T84 cells were seeded in a 48-well plate ($1.5 \times 10^5$ cells per well) and incubated for 1 h with HM or thiazolylaminomannosides **9** and **21**–**31** at final concentrations of 0.1, 1, 10, or 100 $\mu$M. Intestinal cells were then infected for 3 h with the AIEC reference strain LF82 at a multiplicity of infection of 10 bacteria per 1 cell. After washing, infected cells were lysed and samples were diluted and plated onto agar plates to determine the number of colony-forming units (CFU). The effect of mannosides was compared to $\alpha$-D-mannose (D-Man) treatment (100, 1000, 10000, and 50000 $\mu$M). In the absence of any treatment, the adhesion level of AIEC LF82 to T84 cells was


dx.doi.org/10.1021/jm400723n | J. Med. Chem. XXXX, XXX, XXX–XXX

normalized to 100%. The inhibitory ability of mannosides was expressed as a percentage of residual adhesion.

The residual percentages of AIEC LF82 bacteria associated with intestinal epithelial cells T84 in the presence of increasing concentrations of four selected inhibitors (D-Man, HM, **9**, **30**) are presented in Figure 7A (for all the results see Supporting Information Figure S4). All the mannosides tested exerted a dose-dependent inhibitory effect on AIEC LF82 adhesion. α-D-Mannose, HM, and all the compounds tested displayed very large differences when concentration values corresponding to $IC_{50s}$ were considered. For example, similar residual adhesion levels (51.6%, 52.4%, and 57.6%) were observed with 1000 μM of α-D-mannose, 10 μM of HM, and 0.1 μM of compound **30**, respectively (Figure 7A, red bars). The inhibitory potency of compound HM was therefore 100 times greater than that of α-D-mannose, indicating that the antiadhesive effect observed on AIEC bacteria greatly benefits from the anomeric heptyl chain of HM. Importantly, compound **30** exhibited a dose-dependent inhibition similar to HM but at a 100-fold lower concentration (rIC ∼ 0.01). When the residual bacterial adhesion in the presence of antagonists at 1 μM concentration was compared (Figure 7B), the much higher potency of **30** was further evidenced. In fact, no significant decrease in bacterial adhesion was observed with HM at this concentration, while only 14% of AIEC remained attached to the cells when **30** was applied ($p < 0.001$). These results are in good agreement with the previous assays (competitive ELISA and HAI) and show the very strong antiadhesive properties of **30** on AIEC.

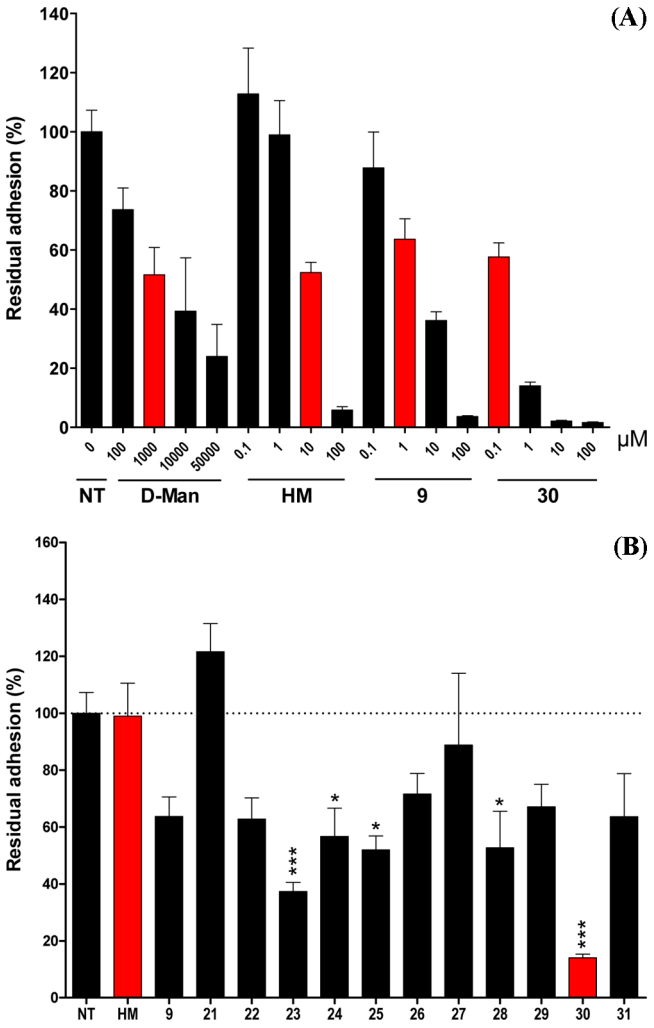


**Figure 7.** (A) Dose-dependent inhibitory effects on the ability of the AIEC strain LF82 to adhere to T84 cells obtained with D-Man, HM, **9**, and **30**. Horizontal scale: concentration of inhibitors expressed in μM. Results are expressed in percentage of bacteria adherent to cells (means ± SEM); 100% corresponds to adhesion in the absence of any treatment (NT for nontreated). (B) Comparison of the inhibitory effects on the AIEC strain LF82 adhesion to T84 cells obtained with HM, **9**, and **21**−**31** at 1 μM concentration. Results are expressed in percentage of bacteria adherent to the cells (means ± SEM); 100% corresponds to adhesion in the absence of any treatment (NT for nontreated). *, $p < 0.05$; **, $p < 0.01$; ***, $p < 0.001$ (One-way ANOVA).

**Prevention of Bacterial Attachment to Colonic Tissue from CEABAC10 Mice: Ex Vivo Assay.** Finally, we explored ex vivo the relative capacity of D-Man and **30** to prevent the adhesion of AIEC bacteria to the gut of FVB/N CEABAC10 transgenic mice (transgenic mouse model mimicking AIEC colonization in CD patients).[25] The mice colons were removed and segmented into four independent loops. A 100 μL solution containing $2 \times 10^5$ AIEC bacteria with or without D-Man (1 μmol and 10 μmol) or compound **30** (0.01 μmol and 0.1 μmol) was injected into the loops and incubated for 1 h within the tissue. After four washes, the residual bacterial adhesion to the gut in the presence or absence of inhibitors was determined after incubation. The adhesion levels normalized to 100% are presented in Figure 8.

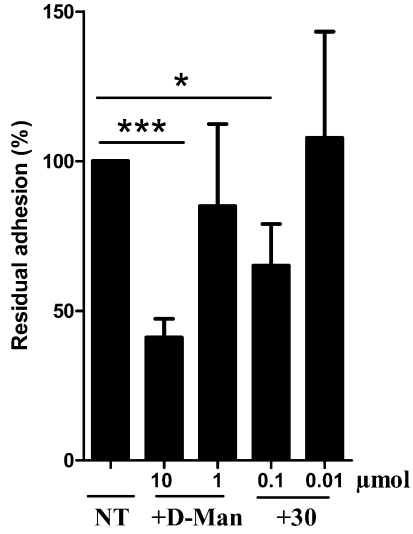


**Figure 8.** Comparison of the inhibitory effects on AIEC bacterial adhesion to the colonic tissue of transgenic CEABAC10 mice obtained with D-Man and **30**. Results are expressed as percentage of bacteria adherent to the colonic mucosa (means ± SEM, $n = 5-8$ mice). 100% corresponds to bacterial adhesion in the absence of treatment (NT for nontreated). *, $p < 0.05$; ***, $p < 0.001$ (one-way ANOVA).

Ten μmol (1.8 mg) of D-Man was shown to decrease the level of residual adhesion to 41%. In comparison, the minimum quantity of compound **30** to give a significant inhibitory effect was much lower, and a residual adhesion of 65% was observed with 0.1 μmol (0.036 mg) of compound. In this assay, compound **30** was therefore 10- to 100-fold more potent than D-Man at preventing AIEC attachment to the colonic mucosa. Lower inhibitory effects, if any, were observed when 10-fold


dx.doi.org/10.1021/jm400723n | J. Med. Chem. XXXX, XXX, XXX−XXX

lower quantities of D-Man (1 μmol, 1.8 mg) and **30** (0.01 μmol, 0.0036 mg) were injected into the loops. These results show a dose-dependent antiadhesive effect and highlight the possibility of decreasing the residual bacterial adhesion further with higher doses of FimH inhibitors.

## CONCLUSION

We have developed here a synthetic methodology to build anomeric heterocycles (pyrimidines and thiazoles) on mannose sugar. This chemical procedure provided access to a new class of FimH inhibitors not reachable by conventional glycosylation reactions. As other sugars can be functionalized by such protocols,[26] this cyclization strategy may not be restricted to the design of FimH inhibitors and is probably applicable to designing sugar antagonists of other biologically relevant lectins.[27,28] In the present case, the thiazolylaminomannosides **9** and **21**−**31** were the only compounds adopting the required $^1C_4$ configuration for an optimal fit in the FimH binding pocket. The pyrimidine derivatives showed a low affinity for the target (result not shown) and were not further considered. The lead compound **9** was shown to interact strongly with FimH in an ELISA assay. The high-resolution crystal structure of the FimH lectin domain with **9** showed the thiazolyl moieties interacting with Tyr48 and Tyr137 of the so-called "tyrosine gate". Insights into the high affinity of **9** for FimH were provided by calculating the interaction energies. The results showed that the thiazole moiety stabilizes the interactions with the two tyrosines more than the widely used phenyl group does.

The parallel but staggered orientation of the thiazole with the aromatic ring of Tyr48 suggested that new pharmacophores replacing the methyl group of **9** would give additional π-stacking with Tyr48. Thus, we developed a small library of analogues mostly based on aromatic compounds. Most of this second generation of thiazolylaminomannosides showed nanomolar affinity for FimH. A cell-based assay revealed for the first time that synthetic mannosides can efficiently prevent the attachment of AIEC bacteria to human intestinal cells. This effect was further evidenced ex vivo in the gut of a transgenic mouse model of CD.[25] As AIEC bacteria are known to colonize the ileal mucosa of patients with CD and to induce gut inflammation, this finding may open the way to a potential antiadhesive treatment of CD.

The high capacity of **30** to prevent AIEC adhesion in vitro and ex vivo compared to HM and α-D-mannose is particularly promising and justifies further evaluations. Moreover, **30** was shown to be noncytotoxic and, interestingly, to abolish the apoptotic effect of FimH for intestinal epithelial cells (Caco2) at the low concentration of 100 nM (see Supporting Information.). Future works will focus on the evaluation of compound **30** in vivo to evaluate whether the strong antiadhesive effect observed on intestinal epithelial cells and in the gut correlates with a subsequent improvement in colitis. This will enable the potency of **30** to be defined for preventing/treating chronic intestinal inflammation in CD patients in which AIEC plays a key role.

## EXPERIMENTAL SECTION

## CHEMISTRY

NMR spectra were recorded at room temperature with a Bruker Avance 300 Ultra Shield or eBruker Avance III 400 spectrometer, and chemical shifts are reported in parts per million relative to tetramethylsilane or a residual solvent peak ($CHCl_3$: $^1H$, $\delta$ = 7.26; $^{13}C$, $\delta$ = 77.2; DMSO-$d_6$: $^1H$, $\delta$ = 2.54, $^{13}C$, $\delta$ = 40.4). Peak multiplicity is reported as: singlet (s), doublet (d), triplet (t), quartet (q), multiplet (m), and broad (br). Peak multiplicity and chemical shifts are reported for α compounds in the case of anomeric mixtures in equilibrium. High resolution mass spectra HRMS were obtained by electrospray ionization (ESI) on a Micromass-Waters Q-TOF Ultima Global or with a Bruker Autoflex III SmartBeam spectrometer (MALDI). Low-resolution mass spectra (MS) were recorded with a Thermo Electron DSQ spectrometer. All reagents were purchased from Acros Organics or Aldrich and were used without further purification. Column chromatography was conducted on silica gel Kieselgel SI60 (40−63 μm) from Merck. Reactions requiring anhydrous conditions were performed under argon. Dichloromethane was distilled from calcium hydride under nitrogen prior to use. Microwave experiments were conducted in sealed vials in commercial microwave reactors especially designed for synthetic chemistry (MultiSYNTH, Milestone). The instrument features a special shaking system that ensures high homogeneity of the reaction mixtures. Optical rotations were measured on a 343 Perkin Elmer at 20 °C in a 1 cm cell in the stated solvent; $[\alpha]_D$ values are given in $10^{-1}$ deg·cm$^2$ g$^{-1}$ (concentration $c$ given as g/100 mL). Compounds tested in vitro were determined to be of >95% purity by inverse phase HPLC (C-18).

**2-[(2,3,4,6-Tetra-*O*-acetyl-α-D-mannopyranos-1-yl)-amino]-4-dimethylamino-1,3-thiazabuta-1,3-diene (7).** *N*,*N*-Dimethylformamide dimethyl acetal (DMFDMA) (1.3 mL, 9.7 mmol, 1.3 equiv) was added to a solution of **6** (3.11 g, 7.66 mmol, 1 equiv) in dichloromethane (300 mL) under argon atmosphere. The mixture was stirred at rt for 3 h. The solvent was evaporated under reduced pressure and the residue purified by chromatography on a silica gel column with petroleum spirit−ethyl acetate (3−7 to 4−6) as eluent to afford **7** (3.32 g, 94%) as a mixture of two conformational isomers A and B. $^1H$ NMR (300 MHz, $CDCl_3$) $\delta$ = 8.82, 8.77 (2 H, 2*s*, H-9, A + B), 7.69 (1 H, d, $J_{7,1}$= 7.8 Hz, H-7 B), 7.44 (1 H, d, $J$ = 6.6 Hz, H-7 A), 6.19 (1 H, dd, $J_{1,2}$ = 2.7 Hz, $J_{1,7}$ = 8.4 Hz, H-1 A), 5.94 (1 H, dd, $J_{1,2}$ = 1.2 Hz, $J_{1,7}$ = 7.8 Hz, H-1 B), 5.35−5.17 (3 H, m, H-2, H-3, H-4), 4.31−4.26 (1-H, m, H-6$_a$), 4.12−3.91 (2-H, m, H-5, H-6$_b$), 3.20, 3.10 (6 H, 2*s*, H-10, H-10′), 2.15, 2.07, 2.05, 2.00 (12-H, m, $CH_3CO$). $^{13}C$ NMR (75 MHz, MeOD): $\delta$ = 196.3, 194.5 (C-8, A + B), 170.6, 170.5, 170.0, 169.7, 169.5, 169.3 ($CH_3CO$, A + B), 163.3, 162.8 (C-9, A + B), 79.6 et 78.3 (C-1, A + B), 70.4, 69.9 (C-5, A + B), 70.0, 68.7 (C-3, A + B), 66.4, 65.9 (C-4, A + B), 62.0 (C-6, A + B), 41.6, 41.5, 36.1, 35.8 (C-10 and C-10′, A + B), 20.9, 20.8 ($CH_3CO$, A + B). HRMS (ES +): found 489.1354, $C_{19}H_{29}N_3O_9SNa$ requires 489.1360.

**General Procedure for the Addition-Cyclizations.** Example for **8**. 1-Chloropropan-2-one (48 μL, 0.709 mmol) and triethylamine (100 μL, 0.740 mmol) were added to a solution of 2-[(2,3,4,6-tetra-*O*-acetyl-α-D-mannopyranos-1-yl)-amino]-4-dimethylamino-1,3-thiazabuta-1,3-diene **7** (161 mg, 0.349 mmol) in dry THF (5 mL). The mixture was stirred at 60 °C for 16 h then diluted in dichloromethane (20 mL) and washed with water (3 × 10 mL). The aqueous layer was extracted with dichloromethane (20 mL). The organic layers were combined, dried over magnesium sulfate, filtered, and evaporated under reduced pressure. The residue was purified by chromatography on a silica gel column with petroleum spirit−


dx.doi.org/10.1021/jm400723n | J. Med. Chem. XXXX, XXX, XXX−XXX

ethyl acetate (1−1) as eluent to afford **8** as a white solid (83%, $\alpha/\beta$ = 9/1).

**5-Acetyl-2-((2,3,4,6-tetra-*O*-acetyl-α-D-mannopyranos-1-yl)amino)thiazole (8).** $\alpha/\beta$ = 4/1. $^1$H NMR (300 MHz, $CDCl_3$) $\delta$ = 9.00 (1 H, br, NH), 7.98 (1 H, s, H-8$_\alpha$), 7.79 (1 H, s, H-8$_\beta$), 5.52 (1 H, dd, $J_{2,1}$ = 1.8 Hz, $J_{2,3}$ = 2.7 Hz, H-2), 5.34−5.24 (2 H, m, H-3, H-4), 5.14 (1 H, d, $J_{1,2}$ = 1.8 Hz, H-1$_\alpha$), 4.32 (1-H, dd, $J_{6b,6a}$ = 12.0 Hz, $J_{6b,5}$ = 5.4 Hz, H-6$_b$), 4.11−4.01 (2 H, m, H-5, H-6$_a$), 2.43 (3 H, s, H-11), 2.18, 2.06, 2.01, 2.00 (12 H, 4 s, $CH_3CO$). $^{13}$C NMR (75 MHz, $CDCl_3$): $\delta$ = 189.8 (C-10), 172.6 (C-7), 170.8, 170.2, 169.7 ($CH_3CO$), 146.7 (C-8), 131.5 (C-9), 82.5 (C-1), 69.4 (C-5 + C-3 or C-4), 69.1 (C-2), 66.0 (C-3 or C-4), 62.2 (C-6), 26.2 (C-11), 20.7 ($CH_3CO$). HRMS (MALDI): found 473.1241, $C_{19}H_{24}N_2O_{10}S$ requires 473.1224.

**2-((2,3,4,6-Tetra-*O*-acetyl-α-D-mannopyranos-1-yl)-amino)-5-(4-methyl-2-(pyrazin-2-yl)thiazole-5-carbonyl)thiazole (19).** $[\alpha]_D$ = +27 ($c$ = 0.4, $CHCl_3$). $^1$H NMR (300 MHz, $CDCl_3$) $\delta$ = 9.45 (1 H, d, $J_{18,17}$ = 1.5 Hz, H-18), 8.65 (1 H, d, $J_{16,17}$ = 2.5 Hz, H-16), 8.55 (1 H, dd, $J_{17,18}$ = 2.5 Hz, $J_{17,16}$ = 1.5 Hz, H-17), 8.12 (1 H, s, H-8), 5.50 (1 H, dd, $J_{2,1}$= 1.8 Hz, $J_{2,3}$ = 2.4 Hz, H-2), 5.40−5.14 (2 H, m, H-1, H-3, H-4), 4.40 (1 H, dd, $J_{6b,6a}$ = 12.9 Hz, $J_{6b,5}$ = 5.7 Hz, H-6$_b$), 4.12−3.99 (2 H, m, H-5, H-6$_a$), 2.75 (3 H, s, H-14), 2.16, 2.07, 2.00, 1.90 (12 H, 4 s, C$H_3$CO). $^{13}$C NMR (75 MHz, $CDCl_3$): $\delta$ = 177.6 (C-10), 172.5 (C-7), 170.8, 170.5, 170.2, 169.7 ($CH_3CO$), 166.7, 160.5 (Car), 147.7 (C-8), 146.1 (C-16), 144.2 (C-17), 142.0 (C-18), 133.1 (C-11) 129.8 (C-9), 82.3 (C-1), 69.8 (C-3 or C-4), 69.1 (C-2), 68.6 (C-5), 66.0 (C-3 or C-4), 62.0 (C-6), 20.7 ($CH_3CO$), 18.8 ($CH_3$). HRMS (ES+): found 634.1263, $C_{26}H_{27}N_5O_{10}S_2$ requires 634.1272.

**General Procedure for the Deprotection.** Example for **9**. A solution of sodium methanolate 0.1 M (60 μL, 1 equiv) was added to a solution of tetra-*O*-acetylmannopyranosylamino-thiazole (138 mg, 1 equiv) in methanol (5 mL), and the mixture was stirred at rt for 3 h. The mixture was diluted with osmosed water (5 mL) and neutralized with Amberlite IRA-120 ($H^+$) ion-exchange resin, filtered, and evaporated under reduced pressure. The residue was chromatographed on a C-18 column with 100−0 to 0−100 water−methanol (linear gradient) as eluent to afford **9**.

**5-Acetyl-2-((α-D-mannopyranos-1-yl)amino)thiazole (9).** $\alpha/\beta$ > 4/1. $^1$H NMR (300 MHz, $D_2O$) $\delta$ = 8.09 (1 H, s, H-8), 5.34 (1 H, s, $J_{1,2}$ = 1.7, H-1$_\alpha$), 4.19 (1 H, dd, $J_{2,1}$ = 1.7 Hz, $J_{2,3}$ = 3.3 Hz, H-2), 3.91−3.46 (5 H, m, H-3, H-4, H-5, H-6), 2.54 (3 H, s, H-11). $^{13}$C NMR (75 MHz, $D_2O$): $\delta$ = 194.1 (C-10), 174.1 (C-7), 149.3 (C-8), 129.2 (C-9), 83.7 (C-1), 73.3, 70.5, 69.6, 66.7, 60.7 (C-2, C-3, C-4, C-5, C-6), 25.3 (C-11). HRMS (MALDI): found 327.06049, $C_{11}H_{16}N_2O_6SNa$ requires 327.06213.

**2-(α-D-Mannopyranos-1-yl)amino)-5-(4-methyl-2-(pyrazin-2-yl)thiazole-5-carbonyl)thiazole (30).** $\alpha/\beta$ > 3/1. $^1$H NMR (400 MHz, $CD_3OD$) $\delta$ = 9.35 (1 H, s, H-18), 8.82 (1 H, d, $J_{16,17}$ = 2.4 Hz, H-16), 8.76 (1 H, d, H-17), 8.00 (1 H, m, H-8) 5.17 (1 H, d, $J_{1,2}$ = 1.8 Hz, H-1), 5.40−5.14 (6 H, m, H-2, H-3, H-4, H-5, H-6). $^{13}$C NMR (100 MHz, DMSO): $\delta$ = 176.4 (C-10), 173.6 (C-7), 165.7, 157.5 (Car), 149.8 (C-8), 146.5 (C-16), 145.2 (Car), 144.7 (C-17), 140.7 (C-18), 130.2, 129.1 (C-9, C-11), 83.4 (C-1), 75.0 (C-5), 70.5 (C-3 or C-4), 69.4 (C-2), 67.1 (C-4 or C-3), 60.9 (C-6), 17.3 ($CH_3$). HRMS (ESI +): found 466.08484, $C_{18}H_{20}N_5O_6S2$ requires 466.08495.

**ELISA.** Immunosorbent microplates were coated with 100 μL of a 10 mg/mL solution of RNaseB in 100 mM carbonate/bicarbonate buffer pH 9.6. Plates were incubated at 4 °C overnight and then washed (300 μL/well) three times with 10 mM phosphate-buffered saline (PBS) containing 0.15% Tween-20. All wells were blocked with 250 μL of 3% bovine serum albumin (BSA) in 10 mM phosphate-buffered saline (PBS) containing 0.15% Tween-20 (PBST), incubated at 37 °C for 2 h then washed three times with PBST. Thiazole-bearing mannosides were dissolved in PBST in the concentrations indicated on graphs and added to microwells. FimH was diluted in PBST to 0.07 μM and added to each plate well then incubated for 1 h at room temperature. Wells were washed three times with PBST before being incubated with 100 μL of rabbit-anti-FimH antibodies IgG (aFimH), diluted 1:2500 in PBST, for 1 h at room temperature. Wells were washed 3 times with PBST and incubated with 100 μL of goat-antirabbit HRP-labeled secondary antibody, Enzo Life Sciences (2ndAb-HRP), diluted 1:5000 in PBST, for 1 h at room temperature. They were then washed three times with PBST and 100 μL of 3,3′,5,5′-tetramethylbenzidine (TMB) was added to each well and incubated in darkness for 2−5 min. The reaction was stopped with 100 μL/well of 1N sulfuric acid. Plate absorbance was analyzed at 450 nm using a BioTek-ELx800 microplate reader.

**Crystal Structure of the FimH Lectin Domain in Complex with 9.** Crystallization was accomplished in two different space groups using the sitting drop vapor diffusion method. The sitting drops were formed by 100 nL of the precipitant solution (Supporting Information Table S2) layered on top of 100 nL of 18 mg/mL FimH lectin domain in 20 mM Na-Hepes at pH 7.4, 150 mM NaCl and complemented with 20 mM **9** just before setup.

**Calculations.** Ligand **9** was optimized at the B3LYP/6-31+G(d,p) level using Gaussian 09. A relaxed potential energy surface scan for the rotation around the C2−C3 bond was calculated as follows: the starting position of the O−C−C−S dihedral angle (1−2−3−4 in the figure) was 0°. This angle was rotated in 36 steps of 10°. For every step, a geometry optimization was performed at the B3LYP/6-31+G(d,p) level.

For ligand **9** and benzene located at the same position as the heterocycle of ligand **9**, the local hardness was calculated on two positions (see figure) as the electronic part of the molecular electrostatic potential divided by twice the number of electrons.[8]

$$\eta(r) = -\frac{V_{el}(r)}{2N}$$

with $N$ the number of electrons and $V_{el}(r)$ the electronic part of the molecular electrostatic potential. The polarizability of benzene and ligand **9** was analytically calculated at the B3LYP/6-311+G(d,p) level. Interaction energies between ligand **9**, (benzene) and Tyr137 and Tyr48 were calculated at the MP2/6-311++G(d,p) level using a basis set superposition error correction with Gaussian 09 (Figure 9).[29]

**Hemagglutinations.** Interaction of *E. coli* FimH adhesins with the glycocalyx of guinea pig erythrocytes forms a cross-linked network in the wells. Glycoconjugates, added in a 2-fold dilution series, prevent the agglutination reaction. The inhibition titer is defined as the lowest concentration of the glycoconjugate at which hemagglutination is still inhibited. LF82 *E. coli* were grown statically overnight in LB at 37 °C, washed three times in ice-cold phosphate-buffered saline, and redissolved. A 2-fold dilution of glycoconjugates with a starting concentration of 1 mM was prepared in 25 μL of 20 mM


dx.doi.org/10.1021/jm400723n | J. Med. Chem. XXXX, XXX, XXX−XXX

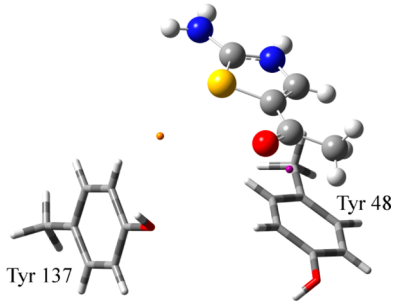


**Figure 9.** Representation of ligand **9** in the mannose-binding site of FimH. The orange and purple dots give the position on which the local hardness was calculated for the interaction with Tyr137 and Tyr48, respectively.

HEPES pH 7.4 with 150 mM NaCl. Importantly, the pipet tip was changed at every dilution step to avoid carry-over. Next, the bacterial solution (25 $\mu$L) was added to the 2-fold dilution series of the compound. Finally, 50 $\mu$L of guinea pig red blood cells, washed and diluted in the buffer to 5% of the blood volume, was added to reach 100 $\mu$L. The plates were left on ice for one night before read-out.

**Adhesion Assays of AIEC LF82 Strain on Intestinal Epithelial Cells T84.** *E. coli* strain LF82 isolated from an ileal biopsy of a CD patient was used as the AIEC reference strain.[3] Bacteria were grown overnight at 37 °C in Luria−Bertani (LB) broth, and a bacterial suspension was prepared at a concentration of $1.5 \times 10^8$ bacteria/mL in phosphate buffer saline (PBS) for adhesion assays.

The human intestinal cell line T84, purchased from American Type Culture Collection (ATCC, CCL-248), was maintained in an atmosphere containing 5% $CO_2$ at 37 °C in the culture medium recommended by ATCC. T84 cells were seeded in 48-well tissue culture plates at a density of $1.5 \times 10^5$ cells/well and incubated at 37 °C for 48 h. Before infection, cells were washed with PBS and incubated for 1 h with HM or thiazole-bearing mannosides at final concentrations of 0.1, 1, 10, or 100 $\mu$M. Effects of mannoside treatment were compared with $\alpha$-D-mannose (D-Man) treatment (100, 1000, 10000, and 50000 $\mu$M). Epithelial cells were then infected in the presence of inhibitory compounds with the AIEC reference strain LF82 for 3 h at a multiplicity of infection (MOI) of 10 bacteria per cell ($1.5 \times 10^6$ bacteria/well). Monolayers were washed three times with PBS and lysed with 1% Triton X-100 (Sigma) in deionized water. Samples were diluted and plated onto LB agar plates to determine the number of colony-forming units (CFU).

**Ex Vivo Assay.** An adhesion assay of AIEC LF82 bacteria was performed using colonic tissue from transgenic mice expressing the human CEACAM6 protein.[25] Briefly, 10−12-week-old FVB/N CEABAC10 transgenic mice were anesthetized and euthanized by cervical dislocation, and colons were removed. Colons were washed twice in phosphate buffer saline (PBS) and segmented into four independent loops of ≈ 0.6 cm. A volume of 100 $\mu$L of LF82 bacteria at $2 \times 10^6$ bacteria/mL in PBS or of a mix of LF82 bacteria + D-mannose (1 $\mu$mol and 10 $\mu$mol) or compound **30** (0.01 $\mu$mol and 0.1 $\mu$mol) was injected into the loops. These were incubated for 1 h at 37 °C in an atmosphere containing 5% $CO_2$ and then opened and washed four times in PBS. Tissues were homogenized, appropriately diluted, and plated onto Luria−Bertani agar plates containing ampicillin (100 $\mu$g/mL) and erythromycin (20 $\mu$g/mL) to select AIEC LF82 bacteria.

## ■ ASSOCIATED CONTENT

### Supporting Information

Experimental procedures and NMR spectra for new compounds. X-ray data collection, data processing, and refinement statistics for FimH−**9** cocrystals and PDB entries 3zl1 and 3zl2. This material is available free of charge via the Internet at http://pubs.acs.org.

### Accession Codes

PDB codes 3zl1 and 3zl2

## ■ AUTHOR INFORMATION

### Corresponding Author

*Phone: +0033 2 51 12 54 06. E-mail: r.bilyy@gmail.com (R.O.B.); Arlette.Darfeuille-Michaud@u-clermont1.fr (A.D-M.); julie.bouckaert@univ-lille1.fr (J.B.); Sebastien.gouin@univ-nantes.fr (S.G.G.).

### Notes

The authors declare no competing financial interest.

## ■ ACKNOWLEDGMENTS

J.B. thanks Andrew Thompson at ProximaI of SOLEIL, Saint Aubin, France, for help with data collection. G.R. acknowledges the FWO for a postdoctoral fellowship. This work was carried out with financial support from the French Agence Nationale de la Recherche (ANR-12-BSV5−0016−01), the Conseil Régional des Pays de La Loire (ERABAC project), the Centre National de la Recherche Scientifique, the Ministère de l'Enseignement Supérieur et de la Recherche in France, the Institut National de la Santé et de la Recherche Médicale (UMR1071), the Institut National de la Recherche en Agronomie (USC INRA 2018), and the Association François Aupetit. The work of T.I.D. and R.O.B. was partially supported by grants from NASU and WUBMRC.

## ■ ABBREVIATIONS USED

AIEC, adherent-invasive *Escherichia coli*; BAC, bacterial artificial chromosome; CD, Crohn's disease; CEA, carcinoembryonic antigen; CEABAC, BAC bearing part of the human CEACAM family gene locus; CEACAM, carcinoembryonic antigen-related cell adhesion molecules; CFU, colony-forming units; DMFDMA, *N*,*N*-dimethylformamide dimethyl acetal; ELISA, enzyme-linked immunosorbent assay; FimH, adhesin portion of type 1 fimbria; HAI, hemagglutination; HM, heptylmannoside; rIC, relative inhibitory concentration; TNF-$\alpha$, tumor necrosis factor- $\alpha$; Tyr, tyrosine; UTIs, urinary tract infections

## ■ REFERENCES

(1) Kaser, A.; Zeissig, S.; Blumberg, R. S. Inflammatory Bowel Disease. *Annu. Rev. Immunol.* **2010**, *28*, 573−621.

(2) Chassaing, B.; Darfeuille-Michaud, A. Commensal microbiota and enteropathogens in the pathogenesis of IBD. *Gastroenterology* **2011**, *140*, 1720−1728.

(3) Darfeuille-Michaud, A.; Neut, C.; Barnich, N.; Lederman, E.; Di Martino, P.; Desreumaux, P.; Gambiez, L.; Joly, B.; Cortot, A.; Colombel, J. F. Commensal microbiota and enteropathogens in the pathogenesis of IBD. *Gastroenterology* **1998**, *115*, 1405−1413.

(4) Darfeuille-Michaud, A.; Boudeau, J.; Bulois, P.; Neut, C.; Glasser, A. L.; Barnich, N.; Bringer, M. A.; Swidsinski, A.; Beaugerie, L.; Colombel, J. F. High prevalence of invasive *Escherichia coli* strains in patients with Crohn's disease. *Gastroenterology* **2004**, *127*, 412−421.

(5) (a) Glasser, A. L.; Boudeau, G.; Barnich, N.; Perruchot, M. H.; Colombel, J. F.; Darfeuille-Michaud, A. Adherent invasive *Escherichia coli* strains from patients with Crohn's disease survive and replicate within macrophages without inducing host cell death. *Infect. Immun.* **2001**, *69*, 5529−5537. (b) Boudeau, J.; Glasser, A. L.; Masseret, E.; Joly, B.; Darfeuille-Michaud, A. Invasive Ability of an *Escherichia coli* Strain Isolated from the Ileal Mucosa of a Patient with Crohn's Disease. *Infect. Immun.* **1999**, *67*, 4499−4509.

(6) Barnich, N.; Carvalho, F. A.; Glasser, A. L.; Darcha, C.; Jantscheff, P.; Allez, M.; Peeters, H.; Bommelaer, G.; Desreumaux, P.; Colombel, J. F.; Darfeuille-Michaud, A. CEACAM6 a receptor of adherent-invasive *Escherichia coli* supports ileal mucosa colonization in Crohn's disease patients. *J. Clin. Invest.* **2007**, *117*, 1566−1574.

(7) Carvalho, F. A.; Barnich, N.; Sivignon, A.; Darcha, C.; Chan, C. H.; Stanners, C. P.; Darfeuille-Michaud, A. *J. Exp. Med.* **2009**, *206*, 2179−2189.

(8) (a) Gouin, S. G.; Wellens, A.; Bouckaert, J.; Kovensky, J. Multimeric heptyl mannosides as potent anti-adhesives of uropathogenic *Escherichia coli*. *ChemMedChem* **2009**, *5*, 749−755. (b) Almant, M.; Moreau, V.; Kovensky, J.; Bouckaert, J.; Gouin, S. G. Clustering of *Escherichia coli* Type-1 Fimbrial Adhesins by Using Multimeric Heptyl α-D-Mannoside Probes with a Carbohydrate Core. *Chem.—Eur. J.* **2011**, *17*, 10029−10038.

(9) (a) Firon, N.; Ofek, I.; Sharon, N. Carbohydrate-binding sites of the mannose-specific fimbrial lectins of enterobacteria. *Carbohydr. Res.* **1983**, *120*, 235−249. (b) Firon, N.; Ofek, I.; Sharon, N. Contribution of hydrophobicity to hemagglutination reactions of *Pseudomonas aeruginosa*. *Infect. Immun.* **1984**, *43*, 1088−1090. (c) Lindhorst, T. K.; Kötter, S.; Kubisch, J.; Krallmann-Wenzel, U.; Ehlers, S.; Kren, V. Effect of *p*-Substitution of Aryl α-D-mannosides on Inhibiting Mannose-Sensitive Adhesion of *Escherichia coli*—Syntheses and Testing. *Eur. J. Org. Chem.* **1998**, 1669−1674. (d) Han, Z.; Pinkner, J. S.; Ford, B.; Obermann, R.; Nolan, W.; Wildman, S. A.; Hobbs, D.; Ellenberger, T.; Cusumano, C. K.; Hultgren, S. J.; Janetka, J. W. Lead Optimization Studies on FimH Antagonists: Discovery of Potent and Orally Bioavailable Ortho-Substituted Biphenyl Mannosides. *J. Med. Chem.* **2010**, *53*, 4779−4792. (e) Sperling, O.; Fuchs, A.; Lindhorst, T. K. Evaluation of the carbohydrate recognition domain of the bacterial adhesion FimH: design, synthesis and binding properties of mannoside ligands. *Org. Biomol. Chem.* **2006**, *4*, 3913−3922. (f) Grabosch, C.; Hartmann, M.; Schmidt-Lassen, J.; Lindhorst, T. K. Squaric Acid Monoamide Mannosides as Ligands for the Bacterial Lectin FimH: Covalent Inhibition or Not? *ChemBioChem* **2011**, *12*, 1066−1074.

(10) (a) Cusumano, C. K.; Pinkner, J. S.; Han, Z.; Greene, S. E.; Ford, B. A.; Crowley, J. R.; Henderson, J. P.; Janetka, J. W.; Hultgren, S. J. Treatment and prevention of urinary tract infection with orally active FimH inhibitors. *Sci. Transl. Med.* **2011**, *3*, 109−115. (b) Klein, T.; Abgottspon, D.; Wittwer, M.; Rabbani, S.; Herold, J.; Jiang, X.; Kleeb, S.; Lüthi, C.; Scharenberg, M.; Bezençon, J.; Gubler, E.; Pang, L.; Smieško, M.; Cutting, B.; Schwardt, O.; Ernst, B. FimH Antagonists for the Oral Treatment of Urinary Tract Infections: From Design and Synthesis to in Vitro and in Vivo Evaluation. *J. Med. Chem.* **2010**, *53*, 8627−8641. (c) Jiang, X.; Abgottspon, D.; Kleeb, S.; Rabbani, S.; Scharenberg, M.; Wittwer, M.; Haug, M.; Schwardt, O.; Ernst, B. Antiadhesion Therapy for Urinary Tract Infections—A Balanced PK/PD Profile Proved To Be Key for Success. *J. Med. Chem.* **2012**, *55*, 4700−4713.

(11) Bouckaert, J.; Zhaoli, Li.; Xavier, C.; Almant, M.; Caveliers, V.; Lahoutte, T.; Weeks, S.; Kovensky, J.; Gouin, S. G. Heptyl α-D-mannosides grafted on a -cyclodextrin core to interfere with *Escherichia coli* adhesion, an in vivo multivalent effect. *Chem.—Eur. J.* **2013**, *19*, 7847−7855.

(12) (a) Dubber, M.; Lindhorst, T. K. Trehalose-Based Octopus Glycosides for the Synthesis of Carbohydrate-Centered PAMAM Dendrimers and Thiourea-Bridged Glycoclusters. *Org. Lett.* **2001**, *3*, 4019−4022. (b) König, B.; Fricke, T.; Wassmann, A.; Krallmann-Wenzel, U.; Lindhorst, T. K. α-Mannosyl Clusters Scaffolded on Azamacrocycles: Synthesis and Inhibitory Properties in the Adhesion of Type 1 Fimbriated *Escherichia coli* to Guinea Pig Erythrocytes. *Tetrahedron Lett.* **1998**, *39*, 2307−2310. (c) Lindhorst, T. K.; Kieburg, C.; Krallmann-Wenzel, U. Inhibition of the type 1 fimbriae-mediated adhesion of *Escherichia coli* to erythrocytes by multiantennary alpha-mannosyl clusters: the effect of multivalency1. *Glycoconjugate J.* **1998**, *15*, 605−613. (d) Kötter, S.; Krallmann-Wenzel, U.; Ehlers, S.; Lindhorst, T. K. Trivalent α-D-mannoside clusters as inhibitors of type-1 fimbriae-mediated adhesion of *Escherichia coli*: structural variation and biotinylation. *J. Chem. Soc., Perkin Trans. 1* **1998**, 2193−2200.

(13) Schwardt, O.; Rabbani, S.; Hartmann, M.; Abgottspon, D.; Wittwer, M.; Kleeb, S.; Zalewski, A.; Smieško, M.; Cutting, B.; Ernst, B. Design, synthesis and biological evaluation of mannosyl triazoles as FimH antagonists. *Bioorg. Med. Chem.* **2011**, *19*, 6454−6473.

(14) (a) Landreau, C.; Deniaud, D.; Reliquet, A.; Meslin, J. C. A facile access to imidazo[2,1-*b*]thiazole and thiazolo[3,2-*a*]pyrimidine derivatives. *Synthesis* **2001**, *13*, 2015. (b) Landreau, C.; Deniaud, D.; Evain, M.; Reliquet, A.; Meslin, J. C. Efficient regioselective synthesis of triheterocyclic compounds: imidazo[2,1-*b*]benzothiazoles, pyrimido[2,1-*b*]benzothiazolones and pyrimido[2,1-*b*]benzothiazoles. *J. Chem. Soc., Perkin Trans. 1* **2002**, *6*, 741. (c) Landreau, C.; Deniaud, D.; Reliquet, A.; Meslin, J. C. From thiourea to bicyclic structures: an original route to imidazo[2,1-*b*]thiazoles, 5*H*-thiazolo[3,2-*a*]-pyrimidines, 7*H*-imidazo[2,1-*b*][1,3]thiazines, and 2*H*,6*H*-pyrimido-[2,1-*b*][1,3]thiazines. *Eur. J. Org. Chem.* **2003**, *3*, 421. (d) Landreau, C.; Deniaud, D.; Meslin, J. C. From Thiourea to Bicyclic Structures: An Original Route to Imidazo[2,1-*b*]thiazoles, 5*H*-Thiazolo[3,2-*a*]pyrimidines, 7*H*-Imidazo[2,1-*b*][1,3]thiazines, and 2*H*,6*H*-Pyrimido[2,1-*b*][1,3]thiazines. *J. Org. Chem.* **2003**, *68*, 4912. (e) Robin, A.; Julienne, K.; Meslin, J. C.; Deniaud, D. Straightforward Pyrimidine Ring Construction: A Versatile Tool for the Synthesis of Nucleobase and Nucleoside Analogues. *Eur. J. Org. Chem.* **2006**, *3*, 634−643. (f) Kikelj, V.; Setzer, P.; Julienne, K.; Meslin, J. C.; Deniaud, D. Synthesis of nucleoside derivatives via heterocyclocondensation reactions. *Tetrahedron Lett.* **2008**, *49*, 3273−3275. (g) Kikelj, V.; Julienne, K.; Meslin, J. C.; Deniaud, D. Original Ring Contraction of Triazine Derivatives to 1,2,4-Thiadiazoles. *Tetrahedron Lett.* **2009**, *50*, 5802−5804.

(15) (a) Kikelj, V.; Grosjean, S.; Julienne, K.; Meslin, J. C.; Deniaud, D. Concerning the Nucleophilic Displacement of a Methylsulfanyl Group on Substituted Pyrimidinones. *Synthesis* **2010**, 2811−2815. (b) Grosjean, S.; Julienne, K.; Triki, S.; Meslin, J. C.; Deniaud, D. Synthesis of nitrogen bicyclic scaffolds: pyrimido [1,2-*a*] pyrimidine-2,6-diones. *Tetrahedron* **2010**, *66*, 9912−9924.

(16) Kühne, M.; Györgydeák, Z.; Lindhorst, T. K. A Simple Method for the Preparation of Glycosyl Isothiocyanates. *Synthesis* **2006**, *6*, 949−951.

(17) Wang, Q.; Fu, J.; Zhang, J. A facile preparation of peracylated α-aldopyranosyl chlorides with thionyl chloride and tin tetrachloride. *Carbohydr. Res.* **2008**, *343*, 2989−2991.

(18) Camarasa, M. J.; Fernández-Resa, P.; García-López, M. T.; De Las Heras, F. G.; Méndez-Castrillón, P. P.; Felix, A. S. A New Procedure for the Synthesis of Glycosyl Isothiocyanates. *Synthesis* **1984**, 509−510.

(19) (a) Robin, A.; Julienne, K.; Raimbault, S.; Meslin, J. C.; Deniaud, D. An Efficient Synthesis of 1-Substituted Uracil Ring Systems and Their Thio Analogues. *Synlett.* **2005**, *18*, 2805−2807. (b) Robin, A.; Julienne, K.; Meslin, J. C.; Deniaud, D. Synthesis of pyridone and pyridine rings by [4 + 2] hetero-cyclocondensation. *Tetrahedron Lett.* **2004**, *45*, 9557−9559.

(20) Bock, K.; Pedersen, C. A study of $^{13}$CH coupling constants in hexopyranoses. *Chem. Soc., Perkin Trans. 2* **1974**, 293−299.

(21) Mignon, P.; Loverix, S.; Steyaert, J.; Geerlings, P. Influence of the $\pi-\pi$ interaction on the hydrogen bonding capacity of stacked DNA/RNA bases. *Nucleic Acids Res.* **2005**, *33*, 1779−1789.

(22) Bouckaert, J.; Berglund, J.; Schembri, M.; De Genst, E.; Cools, L.; Wuhrer, M.; Hung, C.-S.; Pinkner, J.; Slättegård, R.; Zavialov, A.; Choudhury, D.; Langermann, S.; Hultgren, S. J.; Wyns, L.; Klemm, P.; Oscarson, S.; Knight, S. D.; De Greve, H. Receptor binding studies disclose a novel class of high-affinity inhibitors of the *Escherichia coli* FimH adhesin. *Mol. Microbiol.* **2005**, *55*, 441−455.

(23) Prien, J. M.; Ashline, D. J.; Lapadula, A. J.; Zhang, H.; Reinholda, V. N. The high mannose glycans from bovine ribonuclease B isomer characterization by ion trap MS. *J. Am. Soc. Mass. Spectr.* **2009**, *20*, 539−556.
(24) Wellens, A.; Lahmann, M.; Touaibia, M.; Vaucher, J.; Oscarson, S.; Roy, R.; Remaut, H.; Bouckaert, J. The Tyrosine Gate as a Potential Entropic Lever in the Receptor-Binding Site of the Bacterial Adhesin FimH. *Biochemistry* **2012**, *51*, 4790−4799.
(25) Chan, C. H.; Stanners, C. P. Novel mouse model for carcinoembryonic antigen-based therapy. *Mol. Ther.* **2004**, *9*, 775−785.
(26) Pearson, M. S. M.; Robin, A.; Bourgougnon, N.; Meslin, J.-C.; Deniaud, D. An Efficient Route to Pyrimidine Nucleoside Analogues by [4 + 2] Cycloaddition Reaction. *J. Org. Chem.* **2003**, *68*, 8583−8587.
(27) (a) Chen, C.-P.; Song, S.-C.; Gilboa-Garber, N.; Chang, K. S. S.; Wu, A. M. Studies on the binding site of the galactose-specific agglutinin PA-IL from *Pseudomonas aeruginosa*. *Glycobiology* **1998**, *8*, 7−16. (b) Chabre, Y. M.; Giguère, D.; Blanchard, B.; Rodrigue, J.; Rocheleau, S.; Neault, M.; Rauthu, S.; Papadopoulos, A.; Arnold, A. A.; Imberty, A.; Roy, R. *Chem.—Eur. J.* **2011**, *17*, 6545−6562.
(28) Giguère, D.; Sato, S.; St-Pierre, C.; Sirois, S.; Roy, R. Aryl *O*- and *S*-galactosides and lactosides as specific inhibitors of human galectins-1 and -3: role of electrostatic potential at O-3. *Bioorg. Med. Chem. Lett.* **2006**, *16*, 1668−1672.
(29) Frisch, G. W. T. M. J.; Schlegel, H. B.; Scuseria, G. E.; Robb, M. A.; Cheeseman, J. R.; Scalmani, G.; Barone, V.; Mennucci, B.; Petersson, G. A.; Nakatsuji, H.; Caricato, M.; Li, X.; Hratchian, H. P.; Izmaylov, A. F.; Bloino, J.; Zheng, G.; Sonnenberg, J. L.; Hada, M.; Ehara, M.; Toyota, K.; Fukuda, R.; Hasegawa, J.; Ishida, M.; Nakajima, T.; Honda, Y.; Kitao, O.; Nakai, H.; Vreven, T.; Montgomery, Jr. J. A.; Peralta, J. E.; Ogliaro, F.; Bearpark, M.; Heyd, J. J.; Brothers, E.; Kudin, K. N.; Staroverov, V. N.; Kobayashi, R.; Normand, J.; Raghavachari, K.; Rendell, A.; Burant, J. C.; Iyengar, S. S.; Tomasi, J.; Cossi, M.; Rega, N.; Millam, J. M.; Klene, M.; Knox, J. E.; Cross, J. B.; Bakken, V.; Adamo, C.; Jaramillo, J.; Gomperts, R.; Stratmann, R. E.; Yazyev, O.; Austin, A. J.; Cammi, R.; Pomelli, C.; Ochterski, J. W.; Martin, R. L.; Morokuma, K.; Zakrzewski, V. G.; Voth, G. A.; Salvador, P.; Dannenberg, J. J.; Dapprich, S.; Daniels, A. D.; Farkas, Ö.; Foresman, J. B.; Ortiz, V. J.; Cioslowski, D. J. *Gaussian 09*, revision A.1; Gaussian Inc.: Wallingford CT, 2009.